The Role of Relative Humidity in Radiative–Convective Equilibrium

Masahiro Sugiyama, Peter H. Stone, and Kerry A. Emanuel

Program in Atmospheres, Oceans, and Climate, Massachusetts Institute of Technology, Cambridge, Massachusetts

ABSTRACT

The following conditions are derived for the existence of a radiation limit of tropospheric origin in a nongray atmosphere, extending the work on a gray atmosphere by Nakajima et al.: 1) the atmosphere must become sufficiently optically thick, and 2) the temperature must become only a function of optical depth at each frequency, independent of surface temperature. The first condition is satisfied at high temperatures even in a window region as long as there is weak but nonzero absorption, because the optical depth of the entire atmosphere roughly scales as saturation vapor pressure. At high temperatures, the pseudoadiabatic temperature structure asymptotes to the saturation vapor pressure curve, satisfying the second condition at each frequency. A rapidly decreasing vertical gradient of water vapor mixing ratio allows temperature to asymptote faster in optical depth coordinates than in pressure coordinates.

Analyses using a radiative–convective model show that interactive relative humidity can give rise to a different kind of runaway greenhouse effect and multiple equilibria, if the strength of relative humidity feedback exceeds a critical value. The results suggest that this mechanism may be able to explain the runaway greenhouse effect found by Rennó et al. and radiative–convective multiple equilibria by Rennó. The framework employed in this study will serve as a diagnostic tool for further research on the runaway greenhouse effect and radiative–convective multiple equilibria.

1. Introduction

Radiative–convective models, originally developed by Manabe and Strickler (1964) and subsequently extended by numerous researchers, have helped us understand the vertical structure and heat balance of the atmosphere. Nowadays, they have evolved into single-column models by incorporating various physical processes, and serve as laboratories for testing parameterizations (Jakob 2003; Randall et al. 2003).

This type of model has also facilitated research on the runaway greenhouse effect, a concept relevant to the evolution of the atmosphere of Venus and Earth (e.g., Ingersoll 1969; Pollack 1971; Kasting 1988; Abe and Matsui 1988). On a planet where the amount of greenhouse gas is temperature dependent, there exists an upper bound to the terrestrial emission. The limit to the radiation originates from two mechanisms: stratospheric conditions (Komabayashi 1967; Ingersoll 1969) and tropospheric conditions (Simpson 1927; Abe and

Matsui 1988; Kasting 1988; Nakajima et al. 1992).[1] We may call these upper limits the stratospheric and tropospheric radiation limits, respectively. Once the solar forcing exceeds the smaller of the two, the temperature would continue to increase until all the liquid phase of the greenhouse gas evaporates. This idea has also been employed in a local sense to explain the radiation and heat balance in Earth's Tropics (Pierrehumbert 1995).

Pioneering investigators of the stratospheric radiation limit utilized gray radiative equilibrium models and analytically found conditions for the radiation limit (Komabayashi 1967; Ingersoll 1969). The stratospheric radiation limit is called the Komabayashi–Ingersoll limit after these two authors. Radiative–convective models with detailed radiation calculations also show a radiation limit, but its cause was not well known until the work by Nakajima et al. (1992), who first distin-

Corresponding author address: Masahiro Sugiyama, 77 Massachusetts Avenue, Room 54-1715, Cambridge, MA 02139.
E-mail: masahiro@mit.edu

[1] Some authors classify Simpson's work as one on the stratospheric radiation limit (e.g., Rennó 1997; Pujol and North 2002). However, he utilized a fixed temperature structure instead of assuming a radiative equilibrium, and found an asymptotic radiation limit (see his Figs. 1 and 2). Therefore we categorize his work as one concerning the tropospheric radiation limit.

guished the two radiation limits and identified the physical mechanism underlying the tropospheric radiation limit as an asymptoting temperature structure. They did not, however, formulate the conditions for the radiation limit analytically, and their analysis was restricted to a gray case. Ishiwatari et al. (2002) have performed numerical experiments with a three-dimensional general circulation model, and found an upper bound to solar forcing with which the atmosphere can reach an equilibrium state, which approximately corresponds to the radiation limit calculated from a static radiative–convective model.

Although it has been traditionally assumed that a radiative–convective model possesses a single equilibrium state (Manabe and Strickler 1964; Manabe and Wetherald 1967; Ramanathan and Coakley 1978), some recent work has demonstrated multiple equilibrium solutions. Rennó (1997) found multiple equilibria in a radiative–convective model with an interactive hydrological cycle (relative humidity). A notable difference between the two equilibria appears in the relative humidity profile: one is similar to that found in the Tropics and the other is saturated, although Rennó did not fully address the cause of the multiple equilibria. Pujol and North (2002) demonstrated multiple equilibria in their radiative–convective model that includes semigray radiation; however, they note that their model does not yield multiple equilibria under earth-like conditions. Pujol (2002) and Pujol and North (2003) also examined the effect of semigray radiation in a radiative equilibrium model. Pujol and Fort (2002) analyzed the influence of the atmospheric absorption of sunlight.

The multiple equilibria found by Rennó (1997) and Pujol and North (2002) are due solely to the properties of convection and radiation, independent of the surface albedo feedback. The effect of surface albedo feedback has been examined by Wang and Stone (1980) and Li et al. (1997). Ide et al. (2001) found bimodal solutions for optical properties of the atmosphere in their pure radiative model.

Among the research on the runaway greenhouse effect and multiple equilibria, Rennó et al. (1994) and Rennó (1997) are distinct in that they have calculated relative humidity interactively. Rennó et al. (1994) found that their atmosphere runs away at much lower temperatures (presumably with much lower opacity than other investigators). Kelly et al. (1999) also used a radiative–convective model with an explicit hydrological cycle but in a highly parameterized way. Nevertheless, these authors have not fully explained the physical role of relative humidity in a radiative–convective model. In this paper, we examine how relative humidity affects the radiation limit and the existence of multiple equilibria, with the aim of interpreting the results of Rennó et al. (1994) and Rennó (1997).

Our approach is simple: we do not attempt to calculate relative humidity from prognostic equations or a parameterization, nor do we address the processes

characterizing relative humidity. Instead, we thoroughly examine the potential role of the relative humidity feedback. Our goal here is to illustrate the potential effect of interactive relative humidity and to provide a framework for analyzing such an effect, rather than to document the result of a particular kind of parameterization or system of simplified, balanced equations. With this framework, we present a tentative explanation for the findings of Rennó et al. (1994) and Rennó (1997).

The organization of this paper is as follows: section 2 analytically derives the conditions for the tropospheric radiation limit. Section 3 examines the effect of interactive relative humidity both in gray and nongray models. The paper concludes with discussion in section 4.

2. Conditions for the tropospheric radiation limit

a. Derivation

We begin with the derivation of the conditions for the tropospheric radiation limit. We consider a radiative–convective equilibrium that would develop in response to a prescribed surface temperature and evaluate the outgoing longwave radiation (OLR) in this equilibrium. The equation for the upward monochromatic radiation flux density can be written as (e.g., Goody and Yung 1989; Liou 2002)

$$\mu_0 \frac{dF_\nu^+}{d\tau_\nu} = F_\nu^+ - \pi B_\nu,$$

within the two-stream/Eddington approximation, neglecting scattering. Here, F_ν^+ is the upward radiation flux density, B_ν is the Planck function, τ_ν is the normal optical depth, μ_0 is the cosine of the zenith angle, and the subscript ν denotes frequency. Since temperature in this model is a function of any vertical coordinate and surface temperature [e.g., $T = T(\tau_\nu, T_s)$], we write the general solution for the radiation flux density at the top of the atmosphere with a blackbody surface as

$$F_{\nu,t}^+ = \pi B_\nu(T_s) \exp\left[-\frac{\tau_{\nu,s}(T_s)}{\mu_0} \right]$$
$$+ \int_0^{\tau_{\nu,s}(T_s)} \pi B_\nu[T(\tau_\nu', T_s)] \exp\left(-\frac{\tau_\nu'}{\mu_0} \right) \frac{d\tau_\nu'}{\mu_0},$$

(1)

where T is temperature and the subscripts s and t denote surface and the top of the atmosphere, respectively. The first term represents emission from the surface while the second term signifies the atmospheric emission. This solution is valid also for $\tau_{\nu,s} = 0$ (the atmosphere is transparent at this frequency) as the second term vanishes and the exponential factor in the first term becomes one.

Differentiating (1) and applying the Leibniz theorem leads to

$$\frac{dF_{\nu,t}^{+}}{dT_s} = \frac{d\pi B_\nu(T_s)}{dT_s} \exp\left[-\frac{\tau_{\nu,s}(T_s)}{\mu_0}\right] - \frac{\pi B_\nu(T_s) - \pi B_\nu[T(\tau_{\nu,s}(T_s), T_s)]}{\mu_0} \exp\left[-\frac{\tau_{\nu,s}(T_s)}{\mu_0}\right] \frac{d\tau_{\nu,s}(T_s)}{dT_s}$$

$$+ \int_0^{\tau_{\nu,s}(T_s)} \frac{\partial\{\pi B_\nu[T(\tau_\nu', T_s)]\}}{\partial T_s} \exp\left(-\frac{\tau_\nu'}{\mu_0}\right) \frac{d\tau_\nu'}{\mu_0}. \tag{2}$$

The surface temperature T_s can be different from the temperature right above the surface $T[\tau_{\nu,s}(T_s), T_s]$, although for simplicity we assume no temperature gap at the surface hereafter. Because OLR $\bar{F}$ is the radiation flux density integrated over frequencies, $\bar{F} = \int F_{\nu,t}^+ \, d\nu$, the conditions for the radiation limit, $d\bar{F}/dT_s \to 0$, are

$$\frac{d\pi B_\nu(T_s)}{dT_s} \exp\left[-\frac{\tau_{\nu,s}(T_s)}{\mu_0}\right] \to 0 \quad \text{and}$$

$$\frac{\partial\{\pi B_\nu[T(\tau_\nu, T_s)]\}}{\partial T_s} \to 0 \text{ for all } \nu. \tag{3}$$

The latter condition is equivalent to $T(\tau_\nu, T_s) \to \mathrm{T}(\tau_\nu)$. The former is achieved when the total optical depth of the atmosphere becomes large at high surface temperatures, which is satisfied as long as there is nonzero absorption at the frequency in question, except in the case of extremely weak absorption.[2] That is, even in a window region such as the water vapor window, the surface emission cannot reach space at very high temperatures because of a rapid increase in $\tau_{\nu,s}$. This is because $\tau_{\nu,s}$ roughly scales as saturation vapor pressure:

$$\tau_{\nu,s} = \sum_i \int_0^{p_s} k_\nu^{(i)} r_i \frac{dp}{g} \geq \bar{k}_\nu^{(\upsilon)} \int_0^{p_s} r_\upsilon \frac{dp}{g} \simeq \bar{k}_\nu^{(\upsilon)} r_\upsilon \frac{p_s}{g}$$

$$\simeq \frac{\bar{k}_\nu^{(\upsilon)} e^*(T_s)}{g},$$

where k_ν is the absorption coefficient at frequency ν, the superscript (i) and subscript i imply species i, $r_i \equiv \rho_i/\rho$ is the mixing ratio, ρ is the density, p is the total pressure, g is the acceleration due to gravity, $\bar{k}_\nu^{(\upsilon)} \equiv (\int_0^{p_s} k_\nu^{(\upsilon)} r_\upsilon \, dp/g)/(\int_0^{p_s} r_\upsilon \, dp/g)$, the superscript (υ) and subscript υ denote water vapor, and $e^*(T)$ is the saturation vapor pressure of water. Here, we have assumed that the vertical gradient of the mixing ratio is weak, and that the mixing ratio is close to the mole fraction. As discussed below, the vertical gradient of mixing ratio becomes very weak at high T_s. Further, the difference between mole fraction and mixing ratio becomes small as both of them approach to 1 at high T_s. Thus, if $\bar{k}_\nu^{(\upsilon)}$ changes slowly with surface temperature, the exponential factor in the first condition of (3) scales as $\sim\exp[-\bar{k}_\nu^{(\upsilon)} e^*(T_s)/(\mu_0 g)]$, which rapidly approaches

---

[2] For extremely weak absorption, the temperature would reach the critical point of water before the atmosphere becomes optically thick enough, thereby preventing further increase in optical depth of the entire atmosphere.

zero owing to its double exponential dependence, unless the absorption is zero or extremely weak.

Next, we demonstrate that $T(p, T_s) \to T(p)$ together with $x_i(p, T_s) \to x_i(p)$ is a sufficient condition for $T(\tau_\nu, T_s) \to T(\tau_\nu)$, where $x_i \equiv p_i/p$ is the mole fraction and p_i is the partial pressure.

In the limit of $T(p, T_s) \to \mathrm{T}(p)$, the equation of state implies $\rho_i = \rho_i[p_i(p, T_s), T(p, T_s)] = \rho_i[x_i(p, T_s)p, T(p, T_s)] \to \rho_i[x_i(p)p, T(p)] = \rho_i(p)$, and hence $r_i[p, T(p, T_s)] \to r_i(p)$. Note that if the relative humidity is constant as in our models, $T(p, T_s) \to T(p)$ is the sufficient condition for $x_i(p, T_s) \to x_i(p)$, since $x_\upsilon(p, T_s) = \mathcal{H}e^*[T(p, T_s)]/p \to \mathcal{H}e^*[T(p)]/p = x_\upsilon(p)$ and $x_d(p, T_s) = 1 - x_\upsilon(p, T_s) \to 1 - x_\upsilon(p) = x_d(p)$. Here, e is the partial pressure of water vapor, the subscript d denotes dry air, and $\mathcal{H} \equiv e/e^*(T)$ is the relative humidity. Therefore, $x_i(p, T_s) \to x_i(p)$ is automatically satisfied in our models, provided that $T(p, T_s) \to T(p)$.

Moreover, we have $k_\nu = k_\nu[p, T(p, T_s)] \to k_\nu[p, T(p)] = k_\nu(p)$; k_ν usually depends on pressure and temperature owing to line broadening, but the relation $T(p, T_s) \to T(p)$ simplifies its dependence. These results allow us to rewrite the optical depth as

$$\tau_\nu(p, T_s) = \int_0^p \sum_i k_\nu^{(i)}[p', T(p', T_s)] r_i[p', T(p', T_s)] \frac{dp'}{g}$$

$$\to \int_0^p \sum_i k_\nu^{(i)}(p') r_i(p') \frac{dp'}{g} = \tau_\nu(p). \tag{4}$$

Combining $T(p, T_s) \to T(p)$ and $\tau_\nu(p, T_s) \to \tau_\nu(p)$, we arrive at $T(\tau_\nu, T_s) \to T(\tau_\nu)$.

Note that the pseudoadiabat asymptotes the saturation vapor pressure curve because as T_s increases, $x_\upsilon^* \to 1$ and $x_d \to 0$, which suggests that $p \to e^*(T) = p(T)$ and $T \to T(p)$. Alternatively, this can be shown by taking the limit of a simple formulation of the pseudoadiabat (Iribarne and Godson 1981; Emanuel 1994):

$$\left(\frac{\partial T}{\partial p}\right) = \frac{\dfrac{R_d T}{pc_{pd}} + \varepsilon \dfrac{x_\upsilon^*}{x_d} \dfrac{L_\upsilon}{pc_{pd}}}{x_d + \varepsilon x_\upsilon^* \dfrac{c_{p\upsilon}}{c_{pd}} + \varepsilon^2 \dfrac{x_\upsilon^*}{x_d} \dfrac{L_\upsilon^2}{R_d T^2 c_{pd}}}$$

$$= \frac{\dfrac{x_d}{1 - x_d} \dfrac{R_d T}{pc_{pd}} + \varepsilon \dfrac{L_\upsilon}{pc_{pd}}}{\dfrac{x_d^2}{1 - x_d} + \varepsilon x_d \dfrac{c_{p\upsilon}}{c_{pd}} + \varepsilon^2 \dfrac{L_\upsilon^2}{R_d T^2 c_{pd}}} \to \left[\frac{de^*(T)}{dT}\right]^{-1}, \tag{5}$$

as $x_d \to 0$ (and hence $p \to e^*$). Here, R is a gas constant, c_p is the specific heat at constant pressure, L_v is the latent heat of vaporization, $\varepsilon \equiv R_d/R_v$, and an asterisk denotes saturation. Equation (5) implies $\partial p/\partial T = de^*(T)/dT$, whose integration yields $p = e^*(T) + [p_s - e^*(T_s)]$. Since $p_s \to e^*(T_s)(x_v^* \to 1)$, we obtain $p = p(T) = e^*(T)$ and $T = T(p)$.

The pseudoadiabatic lapse rate can be used as a reference; one can predict the radiation limit for a moist adiabat or other temperature structures by comparing the two. The tropospheric radiation limit in a nongray case appears because of the asymptoting temperature structure, just as in the gray case (Nakajima et al. 1992). Even when more care is taken in the treatment of thermodynamics, such as treating water as a nonideal gas, the temperature structure resembles the saturation vapor pressure curve (Abe and Matsui 1988; Kasting 1988).

It is interesting that the convergence of $T(\tau_v, T_s) \to T(\tau_v)$ is generally faster than that for $T(p, T_s) \to T(p)$ [i.e., $|(\partial T/\partial T_s)_{\tau_v}| < |(\partial T/\partial T_s)_p|$], even though the latter is considered to be the cause of the former (Fig. 1). To gain insight into this, we consider the following limiting case. If water vapor dominates the opacity, the absorption coefficients slowly change with pressure, and the mole fraction and mixing ratio become independent of height (only a function of T_s), then (see appendix A for the derivation)

$$\left(\frac{\partial T}{\partial T_s}\right)_{\tau_v} = \left(\frac{\partial T}{\partial T_s}\right)_p - \left(\frac{\partial T}{\partial \tau_v}\right)_{T_s}\left(\frac{\partial \tau_v}{\partial T_s}\right)_p$$

$$\to \left(\frac{\partial T}{\partial T_s}\right)_p\left[1 - \left(\frac{1}{r_v}\frac{dr_v}{dT_s}\right)\bigg/\left(\frac{1}{x_v}\frac{dx_v}{dT_s}\right)\right]$$

$$= \left(\frac{\partial T}{\partial T_s}\right)_p \alpha,$$

where

$$\alpha \equiv \frac{1}{1 + 1/[(\varepsilon - 1)x_v]}.$$

Note that $|\alpha| < 1$ for $0 \le x_v \le 1$ and $\varepsilon = 0.622$.

In the special case of $x_v = r_v$ as in the model of Nakajima et al. (1992), $|(\partial T/\partial T_s)_{\tau_v}| \to 0$ in this limit even if $|(\partial T/\partial T_s)_p| \neq 0$. In case $x_v \neq r_v$, a decreasing vertical gradient of mole fraction of water vapor combined with dominance of water vapor in opacity still makes the convergence in optical depth coordinates faster than in pressure coordinates. As Ingersoll (1969) showed, the vertical profile of the water vapor mixing ratio in a water vapor-dominated atmosphere is quite different from that in earth-like conditions. The mixing ratio in the latter decreases exponentially with height while that in the former decays slowly.

In summary, the conditions for the tropospheric radiation limit ($d\bar{F}/dT_s \to 0$) are 1) that the atmosphere must be optically thick enough for the surface emission

not to reach the top of the atmosphere; and 2) that temperature must become dependent only on pressure and independent of surface temperature so that the atmospheric emission is fixed.

Physically speaking, the planetary albedo should also converge to a certain value as shown by Kasting (1988). Since (4) applies to the shortwave radiation as well if the absorption coefficient is replaced with an extinction coefficient, then if the atmosphere becomes optically thick enough, the planetary albedo would be independent of the surface albedo and solely determined by the Rayleigh scattering and solar absorption.

b. Illustration using a gray model

We illustrate here how our conditions are satisfied in a simple gray radiative–convective model for the reader's convenience, although the key results have been reported by Nakajima et al. (1992). We use the radiative–convective model of Nakajima et al. (1992); readers can refer to that paper for details. The following summarizes the key features of the model.

The model assumes a radiative–convective equilibrium, and calculates OLR as a function of specified surface temperature. The model atmosphere consists of two components, water vapor-like "condensable" and dry air-like "noncondensable" gases, both of which have the same molecular weight for simplicity. The atmosphere is assumed to be gray, each component having a constant absorption coefficient. The tropospheric lapse rate is pseudoadiabatic, and the stratosphere is in radiative equilibrium. The tropopause is determined by matching temperatures on both sides, keeping the stratosphere in radiative equilibrium and the troposphere pseudoadiabatic. We assume here that the troposphere is saturated as in the original version, but we relax this assumption in the next section. The relative humidity is assumed to be constant with height. Although Nakajima et al. (1992) mainly focused on the case of $k^{(d)} = 0$, we have set $k^{(d)}$ to 4×10^{-4} m^2 kg^{-1} to suppress a peak in OLR that otherwise appears at $T_s \simeq$ 300 K, where the superscript (d) denotes dry air. Throughout this section, the radiation calculation uses the clear-sky condition and the Eddington approximation. Aside from modifications regarding $k^{(d)}$, $\mathcal{H}$, and surface pressure (see the discussion concerning the minimum value of relative humidity below), all model parameters are exactly identical to the standard version of Nakajima et al.'s model.

Figure 1 shows temperature in both pressure and optical depth coordinates along with the vertical profile of the mole fraction for various surface temperatures. The left panel of Fig. 2 describes OLR as a function of surface temperature. The OLR reaches its limit at $T_s \simeq$ 350 K. Turning to Fig. 1, we find that at this surface temperature, T has become a function of only τ, independent of T_s. As expected, the convergence of $T(\tau, T_s) \to T(\tau)$ is faster than that of $T(p, T_s) \to T(p)$ since the
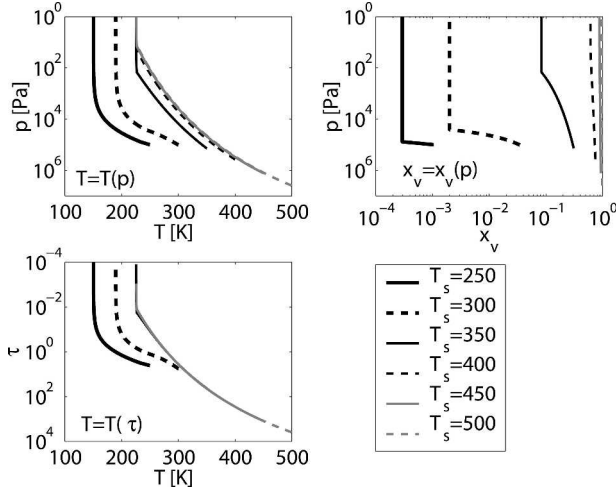
FIG. 1. Vertical profiles of the model atmosphere for the saturated case. (upper left) Temperature in pressure coordinates for different surface temperatures. (lower left) As in upper left but for optical depth coordinates. (upper right) Mole fraction in pressure coordinates. Note that at high temperatures, the temperature structure asymptotes to that of saturation vapor pressure curve. Also notice that the convergence in optical depth coordinates is faster than that in pressure coordinates. Reproduction of Figs. 4 and 5 of Nakajima et al. (1992) but with $k^{(d)} = 4 \times 10^{-4}$ m^2 kg^{-1}.

vertical gradient of x_v decreases rapidly as T_s increases (upper right panel of Fig. 1).

3. Effect of interactive relative humidity

a. A gray model case

Now we begin examining the effect of allowing relative humidity to change interactively by making relative humidity a function of surface temperature. We intro-

duce the phrase "relative humidity feedback" to distinguish interactive relative humidity from conventional "water vapor feedback," which sometimes is taken as constant relative humidity (Held and Soden 2000).

Before looking into the effect of relative humidity feedback, we clarify the existence of a minimum value of relative humidity. In appendix B, we derive the following inequality:

$$\mathcal{H} \geq 1 - \frac{1}{e^*(T_s)} \int_0^\infty \rho_d g \, dz. \tag{6}$$

This arises because in our models, the in-cloud temperature, rather than virtual or density temperature [see chapter 4 of Emanuel (1994) for definitions], is equal to the environment temperature (for more discussions, see appendix B). Equation (6) implies that $\mathcal{H}$ must be larger than a certain positive number if T_s exceeds the boiling point of water at sea level for the current earth. Conversely, inverting this relation yields a maximum temperature for each value of relative humidity.

Although this inequality determines a lower bound to the value of relative humidity, this could be an underestimate because of inequalities involved in the derivation. In all the calculations presented in this paper, we have performed iterations by changing p_d at the surface so that the mass of dry air is conserved. Nakajima et al. (1992) has used a constant p_d at the surface; this is a good approximation if $\mathcal{H} = 100\%$, even when T_s exceeds the boiling point.

The left panel in Fig. 2 shows OLR as a function of surface temperature for various but fixed values of relative humidity. As discussed above, a tropospheric radiation limit appears for the saturated curve ($\mathcal{H} = 100\%$) at $T_s \simeq 350$ K. As $\mathcal{H}$ decreases, the atmosphere becomes more translucent and OLR increases at con-
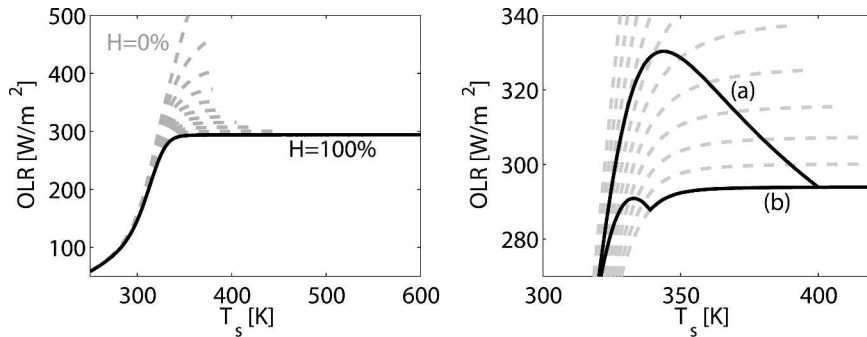
FIG. 2. (left) OLR as a function of surface temperature and constant but different relative humidity, each line representing $\mathcal{H} = 0\%, 10\%, \ldots, 100\%$. Each line is extended to the maximum temperature allowed for each value of relative humidity [see (6) and the subsequent discussion]. (right) OLR as a function of surface temperature when relative humidity is allowed to change interactively $\{\overline{F} = \overline{F}[T_s, \mathcal{H}_i(T_s)]\}$. Lines from the left panel are also shown. The solid line (a) corresponds to $\mathcal{H}_1$, and this hypothetical atmosphere has a new kind of radiation limit. The line (b) corresponds to $\mathcal{H}_2$, which is a stronger function of T_s than $\mathcal{H}_1$, and exhibits multiple equilibria.

stant T_s. Because of (6), the OLR curves for unsaturated cases extend only up to the maximum T_s for each $\mathcal{H}$. The nonzero absorption of the noncondensable component ($k^{(d)} \neq 0$) introduced to suppress a peak in OLR causes different curves to keep very close together at low T_s and the OLR to be very low.

To appreciate the effect of interactive relative humidity, let us conduct a thought experiment. For the sake of argument, we examine two hypothetical atmospheres in which the relative humidity changes with surface temperature as

$$\mathcal{H}_1 = \begin{cases} 20\% & \text{for} \quad T_s \leq 320 \text{ K} \\ 20 + (T_s - 320)\% & \text{for} \quad 320 \text{ K} \leq T_s \leq 400 \text{ K} \\ 100\% & \text{for} \quad 400 \text{ K} \leq T_s \end{cases}$$

and

$$\mathcal{H}_2 = \begin{cases} 20\% & \text{for} \quad T_s \leq 319 \text{ K} \\ 20 + 4(T_s - 319)\% & \text{for} \quad 319 \text{ K} \leq T_s \leq 339 \text{ K} \\ 100\% & \text{for} \quad 339 \text{ K} \leq T_s \end{cases}.$$

This is purely for illustration; such an atmosphere may or may not exist. As a feedback, $\mathcal{H}_2$ especially seems to be too strong. However, this is partly due to the choice of a gray model, and a much weaker feedback is required in a nongray case. We discuss the implications of gray and nongray radiation later.

The line denoted by (a) in the right panel in Fig. 2 describes the OLR in this hypothetical atmosphere, $\overline{F} = \overline{F}[T_s, \mathcal{H}_1(T_s)]$. The radiation limit for this atmosphere happens at $(T_s, \mathcal{H}) \simeq (340 \text{ K}, 40\%)$ although $\overline{F} = \overline{F}(T_s, \mathcal{H} = 40\%)$ does not reach its radiation limit even at the maximum T_s for $\mathcal{H} = 40\%$, indicating that the atmosphere in question runs away despite its low opacity.

The result from including a relative humidity feedback can be understood in terms of (2). In this equation, the only term that can be negative is the last term, which represents the emission from the atmosphere (since in the present case, there is no temperature gap at the surface). Because $(\partial T/\partial T_s)_\tau = -(\partial \tau/\partial T_s)_T/(\partial \tau/\partial T)_{T_s}$ and $\tau \simeq \mathcal{H}[k^{(v)} - k^{(d)}]\int_0^p x_v^* \, dp'/g + k^{(d)}p/g$ (if the stratosphere's contribution is neglected), a sufficiently fast increase in relative humidity with surface temperature causes $(\partial \tau/\partial T_s)_T$ to be positive. Consequently, the last term in (2) becomes negative as $(\partial \tau/\partial T)_{T_s}$ is positive in the troposphere.

An even stronger relative humidity feedback could give rise to multiple equilibria. The curve (b) in Fig. 2b depicts $\overline{F} = \overline{F}[T_s, \mathcal{H}_2(T_s)]$. The model exhibits triple equilibria for a narrow range of OLR from ~288 to ~291 W m^{-2}, suggesting a hysteresis-like response to a change in solar forcing. This narrowness, along with the required strong relative humidity feedback, is a result of our choice of parameters. The middle equilibrium solution might be an unstable branch if the hypothetical atmosphere followed the curve (b) in response to a perturbation, but this may not be the case. Unlike en-
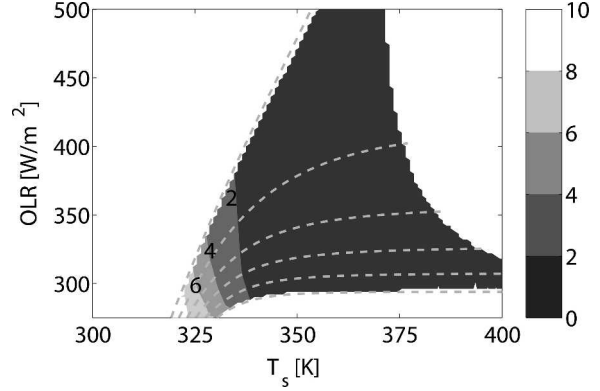
FIG. 3. Critical relative humidity feedback strength necessary for a radiation limit or multiple equilibria $(\partial\mathcal{H}/\partial T_s)_{\overline{F}}$, diagnosed from Nakajima et al.'s (1992) model (shading). The units are % K^{-1}. Dotted lines represent OLR as a function of surface temperature for various, fixed relative humidity, $\mathcal{H} = 0\%, 20\%, \ldots, 100\%$.

ergy-balance models (e.g., North 1975), the present model is not derived by setting the time derivative to zero in a time-dependent equation. Therefore, we cannot employ a linear perturbation analysis, and more knowledge about the system is required to determine its stability (Nakajima et al. 1992).

The difference between the runaway greenhouse effect and multiple equilibria depends on where OLR levels off. If the flattening of OLR occurs below the radiation limit for the saturation case, then there would be multiple equilibria (with two branches having positive sensitivity, $d\overline{F}/dT_s > 0$), since the terrestrial radiation could rise after the atmosphere is saturated. Otherwise, the runaway greenhouse effect would result.

To assess the effect of the relative humidity feedback, we make use of the following relation for $\overline{F} = \overline{F}[T_s, \mathcal{H}(T_s)]$:

$$\frac{d\overline{F}}{dT_s} = \left(\frac{\partial \overline{F}}{\partial T_s}\right)_\mathcal{H} + \left(\frac{\partial \overline{F}}{\partial \mathcal{H}}\right)_{T_s} \frac{d\mathcal{H}}{dT_s}$$

$$= \left(\frac{\partial \overline{F}}{\partial T_s}\right)_\mathcal{H} \left[1 - \frac{d\mathcal{H}}{dT_s} \Big/ \left(\frac{\partial \mathcal{H}}{\partial T_s}\right)_{\overline{F}}\right], \quad (7)$$

where we have applied the implicit function theorem. Equation (7) indicates that if $d\mathcal{H}/dT_s = (\partial\mathcal{H}/\partial T_s)_{\overline{F}}$, then $d\overline{F}/dT_s = 0$. We may call $(\partial\mathcal{H}/\partial T_s)_{\overline{F}}$ the critical relative humidity feedback strength.

The value of the critical feedback strength in the $(T_s, \overline{F})$ plane diagnosed from the model is presented in Fig. 3. It is higher for lower T_s where the atmosphere is far from the radiation limit. It steadily decreases toward zero, converging with the tropospheric radiation limit regime. The implication of this figure is that the atmosphere can run away (or experience a branch transition) anywhere in the $(T_s, \overline{F})$ plane as long as $d\mathcal{H}/dT_s > (\partial\mathcal{H}/\partial T_s)_{\overline{F}}$, is satisfied. Conversely, if $d\mathcal{H}/dT_s < (\partial\mathcal{H}/\partial T_s)_{\overline{F}}$ is

maintained all the time, such an atmosphere would never run away.

b. A nongray model case

The results presented in the prior subsection are from an idealized model developed by Nakajima et al. (1992). In this subsection, we present the critical relative humidity feedback strength from a simple radiative–convective model with the radiation scheme that was formerly used at the European Centre for Medium-Range Weather Forecasts (Fouquart and Bonnel 1980; Morcrette 1991). Morcrette's longwave radiation scheme performs an integration over wavenumbers using a band emissivity method. The longwave spectrum is divided into six spectral regions, including the water vapor continuum band outside the 8–12-μm region, which is essential for the radiation limit [Kasting et al. (1984), see also the discussion on the importance of weak but nonzero absorption above]. Since the curve fitting of transmissivities is done for 180–320 K (Morcrette et al. 1986), we would expect that the resulting values would not be quantitatively reliable for the high temperatures used in this paper. Nevertheless, since calculating the critical relative humidity feedback strength requires many runs of the model, this scheme is computationally efficient enough to provide a useful starting point to estimate the real sensitivity. The choice of this scheme is consistent with a possible future extension of this research; this scheme is implemented in the single-column model of Bony and Emanuel (2001), and it would enable us to compare the results from the time-dependent single-column model with the analyses in the present paper.

We again prescribe an idealized temperature structure. The tropospheric lapse rate is now a moist adiabat [all the way down to the surface; e.g., Eq. (4.7.3) of Emanuel (1994)], and the stratosphere is taken to be isothermal at 200 K, following Kasting (1988). In this subsection, we use the usual molecular weights for water and dry air. Thermodynamic and other parameters are as follows: $c_{pd} = 1005.7$ J kg^{-1} K^{-1}, $c_{pv} = 1870.0$ J kg^{-1} K^{-1}, $c_l = 4218.0$ J kg^{-1} K^{-1}, $R_d = 287.04$ J kg^{-1} K^{-1}, and $g = 9.8$ m s^{-2}. Owing to the large temperature range considered, the same functional form of the saturation vapor pressure curve is used as in the previous subsection, which gives a reasonably good approximation. Accordingly, we have set $L_v = 43\,655/18 \times 10^3$ J kg^{-1} and $R_v = 8.314/18 \times 10^3$ J kg^{-1}. Ozone is excluded from the calculation since it would be destroyed in a warm, moist atmosphere by the by-products of water vapor photolysis (Kasting 1988). The concentration of carbon dioxide is set to 360 ppm. The clear-sky condition is assumed and 300 layers are equally distributed in logarithm of pressure. To ensure conservation of dry air mass, we have performed iterations in a manner similar to that in the gray case.

Figure 4 shows the critical relative humidity feedback strength along with OLR as a function of T_s for various
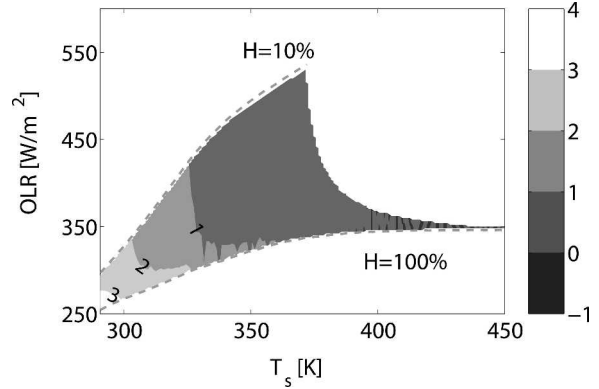
FIG. 4. As in Fig. 3 but for the radiation scheme by Morcrette (1991). Dotted lines correspond to OLR for fixed relative humidities of 10% and 100%.

$\mathcal{H}$. Here, $(\partial \mathcal{H}/\partial T_s)_{\overline{F}}$ obtained from Morcrette's (1991) scheme is much smaller than that for Nakajima et al.'s (1992) model. Again, we see the same tendency as before: the critical values are larger for smaller temperatures where the atmosphere is far away from the radiation limit regime. They decrease as the atmosphere approaches the radiation limit. There are small-scale features in the figure. Since increasing the number of layers from 100 to 300 does not alter the general features, we infer that a further increase in resolution would not significantly alter the outcome.

4. Summary and discussion

Extending the work by Nakajima et al. (1992), we have derived conditions for the existence of the tropospheric radiation limit in a nongray atmosphere. The physics of the radiation limit in a nongray atmosphere is similar to that in a gray atmosphere: 1) the total opacity of the atmosphere is large enough to prevent surface emissions from reaching space; 2) temperature becomes a function of only optical depth at each frequency, thereby fixing the atmospheric emissions regardless of surface temperature. The first condition is satisfied at high surface temperatures because the optical depth of the entire atmosphere scales roughly as saturation vapor pressure. The second condition is attained when water vapor dominates the atmospheric composition at high temperatures, causing the temperature structure to asymptote to the saturation vapor pressure curve. Further, a decreasing vertical gradient of the mole fraction of water vapor accelerates the convergence of temperature in optical depth coordinates, allowing for a rapid appearance of the radiation limit.

In the second part, we have examined the potential effect of including a relative humidity feedback. If relative humidity is allowed to change with surface temperature, then there can be a new kind of radiation limit or multiple equilibria. In order for this to happen, the
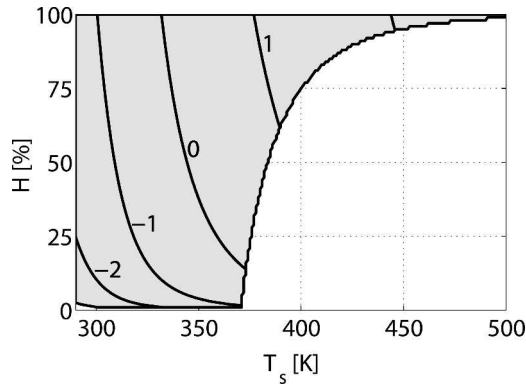
FIG. 5. Pathlength of water vapor as a function of surface temperature and relative humidity. The quantity shown is $\log_{10}(u_v/u_{ref})$, where $u_{ref} = 10^3$ kg m^{-2}. No value is displayed beyond the maximum T_s for each $\mathcal{H}$ (unshaded region). The contour interval is uniform at 1.

relative humidity feedback must be stronger than a critical value. We have diagnosed critical feedback strength for both gray and nongray models.

Having discussed the potential effect of interactive relative humidity, we now turn to the interpretation of the results of Rennó et al. (1994) and Rennó (1997). Rennó et al. (1994) have found that their model atmosphere (unsaturated) with the Goddard Institute for Space Studies (GISS) I and Emanuel convection schemes runs away at a low surface temperature, $T_s \simeq$ 310 K. This temperature is much lower than where the radiation limit is reached in other models that assume saturation, including the ones used here. For instance, the critical temperature for the radiation limit is $T_s \simeq$ 370 K for Kasting (1988) and $T_s \simeq$ 350 K for Pierrehumbert (1995). The effective OLR ($\bar{F}_{eff} = \bar{F}/(1 - \alpha_p)$, where α_p is planetary albedo, which takes into account the albedo effect, does not flatten until $T_s \simeq$ 600 K for Kasting's model. In our case, Fig. 4 shows that OLR levels off at $T_s \simeq$ 400 K.

The difference between their findings and others' suggests that the Rennó et al.'s (1994) model ran away without reaching the conventional tropospheric radiation limit because at low T_s the atmosphere cannot be opaque enough. To confirm this claim, we present an estimate of the pathlength of water vapor, $u_v \equiv \int_0^\infty \rho_v \, dz$, as a surrogate for the optical depth of the entire atmosphere. This gives a rough measure of the opacity, as it is proportional to the optical depth if the absorption coefficient is constant and water vapor dominates the atmospheric opacity ($\tau_{\nu,s} = \int_0^\infty k_\nu^{(v)} \rho_v \, dz = k_\nu^{(v)} u_v$). We use the same model parameters as in the nongray calculations and assume a moist adiabat.

Figure 5 describes the pathlength of water vapor as a function of T_s and $\mathcal{H}$. In the saturation case, we find that u_v increases from $\sim 0.1 \times 10^3$ kg m^{-2} at $T_s = 310$ K to $\sim 10 \times 10^3$ kg m^{-2} at $T_s = 370$ K; u_v decreases with decreasing relative humidity. These two combine to show that the model atmosphere of Rennó et al. (1994)

should be much less opaque than those of other investigators. Consequently, the runaway greenhouse effect in their models cannot be explained by the conventional radiation limits. The cause of the runaway greenhouse in their model might be a strong relative humidity feedback.

Another interesting feature of the relative humidity feedback is that a strong relative humidity feedback can give rise to multiple equilibria. Rennó (1997) found double equilibria for exactly the same boundary condition, but for different initial conditions. Those two equilibria exhibit distinct surface temperatures and relative humidity profiles, one with a Tropics-like profile and another saturated, which corresponds with our analysis.

Yet a more careful analysis is required to exclude the possibility of an artificial runaway greenhouse effect or multiple equilibria in their models. Since the temperature range used in these studies is large, a model may be applied outside its tuning range, resulting in an incorrect outcome. For instance, in a warm, moist atmosphere, moist convection would originate from multiple layers, not only from the boundary layer. Some convection schemes are optimized such that the moist convection originates from the boundary layer, which is a good approximation for earth-like conditions. This simplification, however, would not lead to a correct result if it were used in a study of the runaway greenhouse effect.

The radiation scheme also suffers from problems with a large temperature range. As we mentioned before, the nongray radiation scheme we adopted is not intended for the temperature range we used, which may make our results quantitatively unreliable. In fact, we have compared the planetary albedo from our model with that of Kasting (1988), who carefully designed his radiation scheme to deal with very high temperatures. Kasting's calculation shows that the planetary albedo asymptotes to a certain value as physically expected because the atmosphere should be optically very thick and the albedo would be controlled by the solar absorption and scattering, rather than the surface albedo.[3] On the other hand, our calculations using the radiation scheme by Fouquart and Bonnel (1980) exhibit constantly decreasing albedo (not shown). Thus, we caution that careful attention must be paid to the design of convection and radiation schemes for numerical experiments at extremely high temperatures.

In this paper, we have assumed that relative humidity is constant with height. In nature, however, it exhibits a spatial pattern both horizontally and vertically [e.g., Fig. 6 of Held and Soden (2000)], which may change with surface temperature. Nevertheless, even when a realistic distribution and its change are accounted for,

_____

[3] Kasting cautions that his result may not be reliable since the absorption coefficient for shortwave radiation in his model is derived for only a single temperature.

the main point of our argument that the change in relative humidity can have a significant influence should apply.

Also, note that the magnitude of, and even the sign of, the feedback mechanism should be considered to be state dependent for the large variations used in this paper. The direction and impact of the water vapor feedback could be quite different in a moist, warm atmosphere compared with the present Earth.

We have neglected the cloud feedback, which is probably the most uncertain physical mechanism. Although previous studies note that the cloud albedo effect would dominate in an optically thick atmosphere (Pollack 1971; Kasting 1988; Abe and Matsui 1988; Rennó et al. 1994), how the cloud albedo and greenhouse effects change is yet to be revealed. There are numerous issues involved in determining the cloud feedback, such as cloud microphysical processes and interactions between cloud radiation and large-scale circulations; each of them must be carefully analyzed.

As mentioned in the introduction, our analysis does not use any prognostic equation or balanced equations to determine the relative humidity. Yet the framework we have employed in this paper can be a useful diagnostic tool for research with a prognostic radiative-convective model or a cloud-resolving model.

APPENDIX A

Fast Convergence in Optical Depth Coordinates

We first note that $T(\tau_v, T_s) \to T(\tau_v)$ is equivalent to $(\partial T/\partial T_s)_{\tau_v} \to 0$, which we examine below. This term can be expanded as

$$
\left(\frac{\partial T}{\partial T_s}\right)_{\tau_v} = \left(\frac{\partial T}{\partial T_s}\right)_p - \left(\frac{\partial T}{\partial \tau_v}\right)_{T_s}\left(\frac{\partial \tau_v}{\partial T_s}\right)_p
$$
$$
= \left(\frac{\partial T}{\partial p}\right)_{T_s}\left[-\left(\frac{\partial p}{\partial T_s}\right)_T - \left(\frac{\partial p}{\partial \tau_v}\right)_{T_s}\left(\frac{\partial \tau_v}{\partial T_s}\right)_p\right].
$$
$$(A1)$$

For a fixed relative humidity case, the right-hand side of (A1) can be rewritten by using the following relations:

$$
\left(\frac{\partial p}{\partial T_s}\right)_T = \frac{\partial}{\partial T_s}\left(\frac{\mathcal{H}e^*}{x_v}\right)_T = -\frac{\mathcal{H}e^*}{x_v^2}\left(\frac{\partial x_v}{\partial T_s}\right)_T
$$
$$
= -\frac{p}{x_v}\left(\frac{\partial x_v}{\partial T_s}\right)_T,
$$

$$
\left(\frac{\partial p}{\partial \tau_v}\right)_{T_s}\left(\frac{\partial \tau_v}{\partial T_s}\right)_p = \frac{g}{\sum_i k_v^{(i)} r_i}\int_0^p \frac{\partial}{\partial T_s}\bigg|_{p'}
$$
$$
\left[\sum_i k_v^{(i)}(p', T_s) r_i(p', T_s)\right]\frac{dp'}{g}.
$$

If the opacity is dominated by water vapor ($k_v^{(v)} r_v \gg k_v^{(j)} r_j$ for $j \neq v$),

$$
\left(\frac{\partial T}{\partial T_s}\right)_{\tau_v} = \left(\frac{\partial T}{\partial p}\right)_{T_s}\left\{\frac{p}{x_v}\left(\frac{\partial x_v}{\partial T_s}\right)_T\right.
$$
$$
\left. -\frac{1}{k_v^{(v)} r_v}\int_0^p \frac{\partial}{\partial T_s}\bigg|_{p'}[k_v^{(v)}(p', T_s) r_v(p', T_s)]dp'\right\}.
$$

Moreover, if $k_v^{(v)}(p', T_s)$ slowly changes with p' and T_s, and if we consider the limits of $x_v(p', T_s)$, $r_v(p', T_s) \to x_v(T_s)$, $r_v(T_s)$, then

$$
\left(\frac{\partial T}{\partial T_s}\right)_{\tau_v} \to \left(\frac{\partial T}{\partial p}\right)_{T_s} p\left(\frac{1}{x_v}\frac{dx_v}{dT_s} - \frac{1}{r_v}\frac{dr_v}{dT_s}\right) = \left(\frac{\partial T}{\partial T_s}\right)_p \alpha,
$$
$$(A2)$$

where

$$
\alpha \equiv \frac{1}{1 + 1/[(\varepsilon - 1)x_v]}.
$$

Here, we have used $r_v = \varepsilon x_v/\{1 + (\varepsilon - 1)x_v\}$.

Equation (A2) implies that $(\partial T/\partial T_s)_{\tau_v} \to 0$, if $x_v = r_v$ (i.e., $\varepsilon = 1$) as in the model of Nakajima et al. (1992). In usual cases where $x_v \neq r_v$, taking $\varepsilon = 0.622$, we find that α decreases from 0 to about -0.6 as x_v varies from 0 to 1. Thus, $|(\partial T/\partial T_s)_{\tau_v}| < |(\partial T/\partial T_s)_p|$, and the factor $|\alpha|$ is more effective when the mole fraction is small. Using $x_v \simeq 0.1$ [the value of mole fraction where $T(\tau, T_s) \to T(\tau)$ in Fig. 1] and $\varepsilon = 0.622$ yields $|\alpha| \simeq 0.04$, indicating that the change of temperature in optical depth coordinates is only ~4% of the change in pressure coordinates in this case.

Although the conditions derived above may seem to be overly restrictive, they become very simple in the case of the standard model of Nakajima et al. (1992). Since $k^{(d)} = 0$, $k^{(v)} = $ const, and $x_v = r_v$ in their model, $x_v(p, T_s) \to x_v(T_s)$ only is a sufficient condition for $(\partial T/\partial T_s)_{\tau_v} \to 0$.

APPENDIX B

Minimum Relative Humidity

If the temperature lapse rate is characterized by a saturated ascent (either pseudoadiabatic or moist adiabatic), the total pressure has to be larger than the in-cloud saturation vapor pressure. Under the assumption that virtual temperature is the same inside and outside clouds, this implies

$$p_{d,\text{env}} + \mathcal{H}_{\text{env}}e^*(T_{\text{env}}) = p_{d,\text{cld}} + \mathcal{H}_{\text{cld}}e^*(T_{\text{cld}}) \geq e^*(T_{\text{cld}}),$$

$$\mathcal{H}_{\text{env}} \geq \frac{e^*(T_{\text{cld}})}{e^*(T_{\text{env}})} - \frac{p_{d,\text{env}}}{e^*(T_{\text{env}})}, \qquad \text{(B1)}$$

where $T_{\text{env}}/[1 - (1 - \varepsilon)x_{v,\text{env}}] = T_{\text{cld}}/[1 - (1 - \varepsilon)x_{v,\text{cld}}]$. Here, the subscripts env and cld denote environment and clouds.

On the other hand, we have the following relation for the environment, assuming $\partial r_d/\partial p \leq 0$:

$$\int_0^\infty \rho_d \, dz = \int_0^{p_s} r_d \frac{dp}{g} \geq r_{d,s} \int_0^{p_s} \frac{dp}{g} = \frac{p_{d,s}}{p_{d,s}+\varepsilon e_s} \frac{p_s}{g}$$

$$\geq \frac{p_{d,s}}{g},$$

where p_d is partial pressure of dry air. This allows us to rewrite (B1) as

$$\mathcal{H}_{\text{env}} \geq \frac{e^*(T_{\text{cld}})}{e^*(T_{\text{env}})} - \frac{1}{e^*(T_{\text{env}})} \int_0^\infty \rho_{d,\text{env}}g \, dz. \quad \text{(B2)}$$

This inequality can give a moderate constraint on the value of relative humidity, depending on the temperature difference between clouds and environment.

In our models, for simplicity, we take temperature, rather than virtual temperature, to be the same inside and outside clouds. In addition, relative humidity is constant with height. Under these conditions, evaluating (B2) at the surface yields

$$\mathcal{H} = \mathcal{H}_s \geq 1 - \frac{1}{e^*(T_s)} \int_0^\infty \rho_d g \, dz. \qquad \text{(B3)}$$

This constraint is much stronger than (B2). For moderate surface temperature, the right-hand side is negative and this constraint does not come into play. However, if $e^*(T_s) \geq \int_0^\infty \rho_d g \, dz (\sim 1000 \text{ hPa}$ for earth-like conditions), the right-hand side of (B3) becomes a positive number and there appears a minimum relative humidity.

REFERENCES

Abe, Y., and T. Matsui, 1988: Evolution of an impact-generated H₂O—CO₂ atmosphere and formation of a hot proto-ocean on earth. *J. Atmos. Sci.,* **45,** 3081–3101.

Bony, S., and K. A. Emanuel, 2001: A parameterization of the cloudiness associated with cumulus convection; Evaluation using TOGA COARE data. *J. Atmos. Sci.,* **58,** 3158–3183.

Emanuel, K. A., 1994: *Atmospheric Convection.* Oxford University Press, 580 pp.

Fouquart, Y., and B. Bonnel, 1980: Computation of solar heating of the Earth's atmosphere: A new parameterization. *Beitr. Phys. Atmos.,* **53,** 35–62.

Goody, R. M., and Y. L. Yung, 1989: *Atmospheric Radiation: Theoretical Basis.* 2d ed. Oxford University Press, 519 pp.

Held, I. M., and B. J. Soden, 2000: Water vapor feedback and global warming. *Annu. Rev. Energy Environ.,* **25,** 441–475.

Ide, K., H. L. Treut, Z.-X. Li, and M. Ghil, 2001: Atmospheric radiative equilibria. Part II: Bimodal solutions for atmospheric optical properties. *Climate Dyn.,* **18,** 29–49.

Ingersoll, A. P., 1969: The runaway greenhouse: A history of water on Venus. *J. Atmos. Sci.,* **26,** 1191–1198.

Iribarne, J. V., and W. L. Godson, 1981: *Atmospheric Thermodynamics.* 2d ed. Kluwer Academic, 259 pp.

Ishiwatari, M., S. Takehiro, K. Nakajima, and Y.-Y. Hayashi, 2002: A numerical study on appearance of the runaway greenhouse state of a three-dimensional gray atmosphere. *J. Atmos. Sci.,* **59,** 3223–3238.

Jakob, C., 2003: An improved strategy for the evaluation of cloud parameterizations in GCMs. *Bull. Amer. Meteor. Soc.,* **84,** 1387–1401.

Kasting, J. F., 1988: Runaway and moist greenhouse atmospheres and the evolution of Earth and Venus. *Icarus,* **74,** 472–494.

——, J. B. Pollack, and T. P. Ackerman, 1984: Response of Earth's atmosphere to increases in solar flux and implications for loss of water from Venus. *Icarus,* **57,** 335–355.

Kelly, M. A., D. A. Randall, and G. L. Stephens, 1999: A simple radiative-convective model with a hydrological cycle and interactive clouds. *Quart. J. Roy. Meteor. Soc.,* **125,** 837–869.

Komabayashi, M., 1967: Discrete equilibrium temperatures of a hypothetical planet with the atmosphere and the hydrosphere of one component-two phase system under constant solar radiation. *J. Meteor. Soc. Japan,* **45,** 137–139.

Li, Z.-X., K. Ide, H. Le Treut, and M. Ghil, 1997: Atmospheric radiative equilibria in a simple column model. *Climate Dyn.,* **13,** 429–440.

Liou, K. N., 2002: *An Introduction to Atmospheric Radiation.* 2d ed. Academic Press, 577 pp.

Manabe, S., and R. F. Strickler, 1964: Thermal equilibrium of the atmosphere with a convective adjustment. *J. Atmos. Sci.,* **21,** 361–385.

——, and R. T. Wetherald, 1967: Thermal equilibrium of the atmosphere with a given distribution of relative humidity. *J. Atmos. Sci.,* **24,** 241–259.

Morcrette, J.-J., 1991: Radiation and cloud radiative properties in the European Centre for Medium-Range Forecasts forecasting system. *J. Geophys. Res.,* **96,** 9121–9132.

——, L. Smith, and Y. Fouquart, 1986: Pressure and temperature dependence of the absorption in longwave radiation parameterizations. *Beitr. Phys. Atmos.,* **59,** 455–469.

Nakajima, S., Y.-Y. Hayashi, and Y. Abe, 1992: A study on the "runaway greenhouse effect" with a one-dimensional radiative-convective equilibrium model. *J. Atmos. Sci.,* **49,** 2256–2266.

North, G. R., 1975: Theory of energy-balance climate models. *J. Atmos. Sci.,* **32,** 2033–2043.

Pierrehumbert, R. T., 1995: Thermostats, radiator fins, and the local runaway greenhouse. *J. Atmos. Sci.,* **52,** 1784–1806.

Pollack, J. B., 1971: A nongrey calculation of the runaway greenhouse: Implications for Venus's past and present. *Icarus,* **14,** 295–306.

Pujol, T., 2002: Effects of the non-gray absorption in a simple radiative equilibrium model. *Planet. Space Sci.,* **50,** 1049–1054.

——, and J. Fort, 2002: The effect of atmospheric absorption of sunlight on the runaway greenhouse point. *J. Geophys. Res.,* **107,** 4566, doi:10.1029/2001JD001578.

——, and G. R. North, 2002: Runaway greenhouse effect in a

semigray radiative-convective model. *J. Atmos. Sci.,* **59,** 2801–2810.

——, and ——, 2003: Analytical investigation of the atmospheric radiation limits in semigray atmospheres in radiative equilibrium. *Tellus,* **55A,** 328–337.

Ramanathan, V., and J. A. Coakley Jr., 1978: Climate modeling through radiative-convective models. *Rev. Geophys. Space Phys.,* **16,** 465–489.

Randall, D., and Coauthors, 2003: Confronting models with data: The GEWEX cloud systems study. *Bull. Amer. Meteor. Soc.,* **84,** 455–469.

Rennó, N. O., 1997: Multiple equilibria in radiative-convective atmospheres. *Tellus,* **49A,** 423–438.

——, P. H. Stone, and K. A. Emanuel, 1994: Radiative-convective model with an explicit hydrologic cycle 2. Sensitivity to large changes in solar forcing. *J. Geophys. Res.,* **99,** 17 001–17 020.

Simpson, G. C., 1927: Some studies in terrestrial radiation. *Mem. Roy. Meteor. Soc.,* **16,** 69–95.

Wang, W.-C., and P. H. Stone, 1980: Effect of ice-albedo feedback on global sensitivity in a one-dimensional radiative-convective climate model. *J. Atmos. Sci.,* **37,** 545–552.